Current Research in Food Science 10 (2025) 100949

Contents lists available at ScienceDirect

Current Research in Food Science

journal homepage: www.sciencedirect.com/journal/current-research-in-food-science

3D printed cacao-based formulations as nutrient carriers for immune system enhancement

Rachel L. Milliken [a], Aikaterini Dedeloudi [a], Emily Vong [a], Robyn Irwin [a], Sune K. Andersen [b], Matthew P. Wylie [a,**], Dimitrios A. Lamprou [a,*]

[a] School of Pharmacy, Queen's University Belfast, 97 Lisburn Road, Belfast, BT9 7BL, UK
[b] Janssen Pharmaceutica, Research & Development, Turnhoutseweg 30, 2340, Beerse, Belgium

ARTICLE INFO

Keywords:
Cacao
Honey
VitD3
3D printing
Antibacterial activity
Nutrient administration

ABSTRACT

This study explores the feasibility of using raw Greek honey-infused cacao-based formulations for three-dimensional printing (3DP). It evaluates their physicochemical properties, thermal stability, and rheological behaviour. Three honey varieties, one of which was Lavender Honey (LH), were incorporated into cacao printlets to assess their impact on structural integrity and compatibility with Vitamin D3 (VitD3), a bioactive compound known for immune system enhancement. Including honey aims to improve the nutritional profile, enhance the taste, and potentially increase the bioavailability of VitD3, which is limited by its hydrophobic nature and low oral absorption. Thermal analysis showed that honey-infused cacao printlets maintain a liquid-like state under ambient conditions and exhibit stability up to the printing temperature of 38 °C. Rheological assessments demonstrated that both individually and in combination, increased honey concentrations and VitD3 incorporation enhance viscosity. These changes improve printability and structural integrity during 3DP. While raw LH demonstrated antibacterial activity, no antibacterial efficacy was observed in the LH-based printlets after incubation. LH at a 10% concentration emerged as the optimal formulation, demonstrating balanced structural properties and effective miscibility with VitD3.

This study highlights how raw Greek honey produced without chemical miticides, has the potential to enhance the functionality and palatability of 3D-printed health supplements. It utilises honey's antimicrobial properties and taste benefits while promoting immune system support through VitD3 integration. The findings highlight the versatility of honey-infused cacao printlets in developing personalized health supplements and pharmaceuticals, suggesting their promising role as delivery systems in personalized medicine. Honeys widely accepted sensory qualities and its application in food products are the basis for the proposition that it enhances palatability. These attributes imply that honey could positively influence the acceptability of the product.

1. Introduction

Innovative approaches to maximize the delivery of essential nutrients – those that the body cannot synthesize in sufficient quantities, such as vitamins, minerals, and amino acids, have emerged in recent years due to the combination of nutritional science and technological breakthroughs. Among these, VitD3 stands out with a wide range of health implications, from immune system regulation to skeletal health. Palatability problems and variation in bioavailability are two common problems with traditional supplement delivery techniques, highlighting the need for innovative solutions (Lester et al., 2022; Pressman et al., 2017; Šimoliūnas et al., 2019). Food-based materials like cacao, honey,

Abbreviations: 3DP, three-dimensional printing; VitD3, vitamin D3; CAD, computer-aided design; VH, Vitex honey; LH, *Lavandula angustifolia*; BH, Base honey; PMS, premenstrual syndrome; DSC, Differential scanning calorimetry; FTIR, Fourier-transform infrared spectroscopy; HPLC, high-performance liquid chromatography; MHB, Mueller Hinton Broth; MIC, minimum inhibitory concentration; MBC, minimum bactericidal concentration; CFU, colony forming unit; MH, Mueller Hinton; SD, standard deviation; *S. aureus*, *Staphylococcus aureus*; *E. coli*, *Escherichia coli*; API, active pharmaceutical ingredient; IU, International Units; SDS, Sodium dodecyl sulfate; HSD, Tukey's honestly significant difference test; MHA, Mueller Hinton Agar; QSRS, Quarter Strength Ringers Solution; PBS, Phosphate Buffered Saline; ND, not determined.

* Corresponding author.
** Corresponding author.
E-mail addresses: m.wylie@qub.ac.uk (M.P. Wylie), d.lamprou@qub.ac.uk (D.A. Lamprou).

https://doi.org/10.1016/j.crfs.2024.100949
Received 6 August 2024; Received in revised form 21 November 2024; Accepted 5 December 2024
Available online 9 December 2024

and milk serve as multifunctional excipients, due to their complex compositions, which include polyphenols, proteins, carbohydrates, and lipids. These components offer both nutritional benefits and enhanced drug delivery properties and can mask the taste of active pharmaceutical ingredients (APIs), making medications more appealing, especially for children (Synaridou et al., 2020).

Three-dimensional printing (3DP) technology provides a promising approach for manufacturing tailor-made medications. The versatility of 3DP technology allows the creation of various 3D shapes, from simple structures to engaging cartoon characters, thereby increasing their appeal (Karavasili et al., 2020). Furthermore, 3DP offers significant advantages, including precise dose control, on-demand production, and the ability to fabricate complex dosage forms tailored to individual patient needs, making it a promising method for personalized medicine and nutrient delivery (Eswaran et al., 2023).

Health advantages associated with chocolate have been acknowledged for numerous years. When chocolate is consumed in moderation, especially types with a high cacao content, it has been linked to several potential health benefits. Chocolate consists mainly of flavonoids (Oracz and Żyżelewicz, 2020), which act as antioxidants, enhancing the neutralization of free radicals and subsequently preventing cellular damage in the body (Waterhouse et al., 1996). These flavonoids are proven to have various health benefits, such as improvement of blood flow, reduction of blood pressure, and lower risk of cardiovascular disease (Ullah et al., 2020). Cacao flavonoids can potentially improve neurocognitive functions, enhancing memory and learning skills (Scholey and Owen, 2013). Furthermore, chocolate is known to possess mood enhancing properties by stimulating the release of endorphins and serotonin precursors, which may contribute to a sense of well-being along with lowering stress levels (Parker et al., 2006). However, it is important to note that excessive consumption of chocolate, particularly in varieties with high sugar content, may provoke adverse effects, such as acne, obesity, diabetes, etc. Therefore, selecting chocolate with a high cacao content (e.g., cacao liquor), is crucial to maximize the health benefits and minimize potential adverse effects (Halib et al., 2020).

The application of 3DP technology for cacao-based dosage forms emerges as a viable and advantageous alternative to the traditional mould-casting approach. Traditional chocolate moulds often require significant manual labour and are limited in their ability to produce intricate designs. In contrast, 3DP offers significant benefits such as increased efficiency and accuracy, which is achieved through straightforward adjustments to the parameters of computer-aided design (CAD) models, enabling precise control over the shape and size of the cacao-based products (Chachlioutaki et al., 2022). Additionally, 3DP supports sustainability efforts by reducing material waste and energy consumption, as it allows for the precise deposition of materials, minimizing excess. Thus, the integration of 3DP not only enhances production capabilities but also contributes to more sustainable manufacturing practices (Weaver et al., 2022).

Incorporating honey into 3D-printed cacao-based dosage forms presents a promising avenue for enhancing both flavour and patient compliance. In addition to its appealing taste, honey offers antimicrobial properties due to the presence of various enzymes that produce hydrogen peroxide (H_2O_2) in situ (Brudzynski et al., 2011). This natural component effectively combats various bacterial species, including Streptococcus spp, which can cause serious infections within the digestive system (Brudzynski, 2020). Honey's antimicrobial properties are due to the enzymatic production of hydrogen peroxide, alongside bioactive compounds like polyphenols and flavonoids (Bizerra et al., 2012).

Vitex honey (VH) contains nectar from the chaste tree Jerusalem sage, and thyme (Fig. 1 supplementary material). *Vitex* species are well known in pharmacology to acquire medicinal efficacy, such as anti-inflammatory, antibacterial, antifungal, antimicrobial, antioxidant, and anticancer properties. The nectar from these plants is rich in various bioactive compounds, including terpenes, polyphenols, and flavonoids. Specifically, the major constituents in *V. agnus-castus* are flavonoids (such as casticin, quercetagetin and isovitexin), essential oils, diterpenes, and glycosides (Zahid et al., 2016). These flavonoids have been shown *in vitro* to affect oestrogen receptors, acting as both agonists and antagonists, thus regulating hormonal imbalances (Ramesh et al., 2021). The presence of phytochemical and pharmacological activities of *V. agnus-castus* indicates that *Vitex* honey has the potential for the development of medications for the treatment of hormonal acne, menstrual irregularities, premenstrual syndrome (PMS), and infertility (Kamal et al., 2022). *Lavandula angustifolia* honey (LH) contains nectar from white lavender, Jerusalem sage, and thyme. White lavender is known for its promising potential for reducing anxiety, due to its high levels of tyrosine, a precursor for several other neurotransmitters including dopamine, noradrenaline, and adrenaline (Batiha et al., 2023). Jerusalem sage honey (JH) contains vitamin K, which can assist with faster wound healing and essential oils that provide phenolic compounds with antioxidant and antimicrobial properties ("Jerusalem Sage," n.d.). Similarly, thyme is rich in antioxidants such as thymol, caracrol, lutolin and apigenin and characterized by notable antimicrobial and antibacterial properties (Parham et al., 2020).

Given the promising antimicrobial properties of honey and the phytochemical benefits of *V. agnus-castus,* this study explores the potential of combining these natural ingredients with modern 3DP technology to enhance both therapeutic efficacy and patient compliance. In this study, cacao-based dosage forms enriched with VitD3 were formulated using semi-solid extrusion 3DP. Organic cacao liquor was used as the base, and three varieties of honey – Vitex honey (VH), *Lavandula angustifolia* honey (LH), and Jerusalem sage honey (JH) – were incorporated. The impact of different honey ratios was investigated to enhance both the structural integrity and palatability of the dosage forms, as well as to evaluate their antibacterial potential. This research presents a novel exploration of the thermal, physicochemical, and rheological properties of 3D-printed cacao-based formulations infused with raw honey and VitD3. To the best of our knowledge, no prior studies have explored this combination, making this work a unique contribution to the field.

2. Materials and methods

2.1. Materials

VitD3 (Cholecalciferol, ≥98%), organic cacao paste (100% cacao liquor) were purchased from Sevenhills Wholefoods (England, UK). Raw *Vitex* honey (Euboea Island, Greece), raw *Lavandula angustifolia* honey (Euboea Island, Greece), and Raw Jerusalem sage honey (containing thyme and Jerusalem sage) was provided by Ioannis Argyris beekeeper (Euboea Island, Greece). Acetonitrile, methanol, sodium chloride, sodium dodecyl sulfate (SDS), dipotassium phosphate and hydrochloric acid were purchased from Sigma Aldrich (Dorset, United Kingdom). Mueller Hinton Broth (MHB), Mueller Hinton Agar (MHA), Quarter Strength Ringers Solution (QSRS) and Phosphate Buffered Saline (PBS) were obtained from Oxoid Ltd (Hampshire, UK). Bacterial strains: *Escherichia coli* (ATCC 25922), and *Staphylococcus aureus* (ATCC 29213) were obtained from ATCC (Middlesex, UK) and stored at −80 °C on cryopreservation beads until required.

2.2. Methods

2.2.1. 3D design

The 3DP process was divided into 2 phases: (1) designing and (2) printing. A square with 20 mm × 20 mm x 1 mm dimensions was created using TinkerCAD software and exported as a stereolithography (.stl) file. Choc Print™ software was used to develop and interpret the G-code to produce the printing path required to construct each layer of the 3D geometry. Choc Creator 2.0 Plus® (CHOC EDGE, UK) was used to construct a chocolate sample as illustrated in Fig. 1A depicts the initial

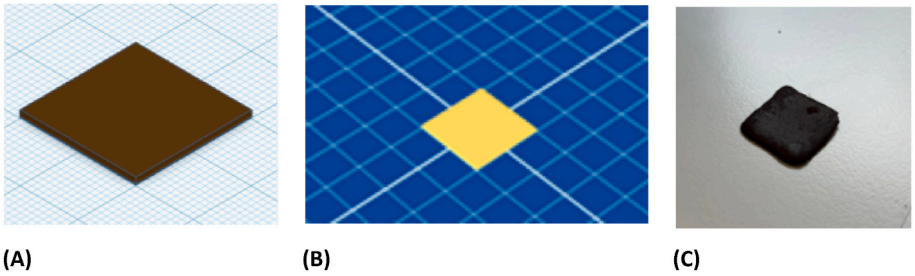

Fig. 1. Graphic illustration of (A) 3D design from TinkerCAD (B) 3D sliced design using Choc Print™ software and (C) 3D printed cacao-based formulation.

3D design from TinkerCAD, (B) shows the sliced design processed by Choc Print™ software, and (C) presents the final 3D printed cacao-based formulation. The dimensions of 20 mm × 20 mm x 1 mm for the geometric design of the 3D cacao-based printlets presented in Table 2, were carefully chosen for several reasons. Firstly, standardizing the dimensions ensures consistency across all printlets, promoting a uniform appearance and size. These dimensions also achieve a practical balance, using less material and printing time while still being large enough for simple handling and observation. The 1 mm thickness allows for controlled portion sizes, facilitating precise dosing of the cacao-based supplements. Ultimately, these dimensions were selected to optimize printing efficiency, ensure product consistency, and meet consumer preferences for bite-sized or portion-controlled products (Benelam and Wiseman, 2019).

2.2.2. 3D printing of cacao-based formulations

For the preparation of 3D cacao-based printlets, cacao was initially melted (T ~ 80 °C). Each honey variant was heated to 37 °C and added to the melted cacao. Two concentrations of honey, 5% and 10% (w/w), were selected to prevent solidification when added to the melted cacao. VitD3 was incorporated into melted cacao (T ~ 80 °C) and gently mixed for 5 min to ensure its complete dissolution in the melted mixture. The concentration of VitD3 used was based on the maximum daily dosage recommended for nutritional intake, which typically ranges from 600 to 800 International Units (IU) per day for adults ("Office of Dietary Supplements - Vitamin D," n.d.). This dosage ensures that the printlets provide an appropriate amount of VitD3 supplementation within the recommended daily allowance. The final cacao-honey-VitD3 formulation was transferred to a water bath maintained at 37 °C and subjected to continuous stirring for 5 min to ensure uniform distribution. The cacao-based ink formulations (as listed in Table 1) were then transferred into the syringe of the chocolate 3D printer (Choc Creator V2.0 Plus®) and extruded at a temperature of 32.5 °C. Subsequently, the printlets were allowed to cool at room temperature.

Table 1
Composition of all cacao-based formulations.

Formulation	Materials (%wt.)				
	Cacao	**VH**	**LH**	**JH**	**VitD3**
F1	100	–	–	–	–
F2	95	5	–	–	–
F3	90	10	–	–	–
F4	95	5	–	–	Incl.
F5	90	10	–	–	Incl.
F6	95	–	5	–	–
F7	90	–	10	–	–
F8	95	–	5	–	Incl.
F9	90	–	10	–	Incl.
F10	95	–	–	5	–
F11	90	–	–	10	–
F12	95	–	–	5	Incl.
F13	90	–	–	10	Incl.

VH: Vitex Honey, LH: Lavender Honey, JH: Base Honey, VitD3: VitD3. Incl.: Included.

Table 2
Mass and dimensions (thickness, width, and length) of cacao-based 3D printed inks containing vitamin D3, cacao, and honey varieties.

Formulation	Weight (mg)	Length (mm)	Width (mm)	Thickness (mm)
F2	593.26 ± 38.75	22.16 ± 0.29	22.09 ± 0.54	1.38 ± 0.16
F3	584.43 ± 94.45	22.05 ± 0.25	22.32 ± 0.40	1.39 ± 0.26
F4	528.00 ± 10.78	21.91 ± 0.41	21.76 ± 0.29	1.49 ± 0.10
F5	554.13 ± 37.07	21.65 ± 0.30	21.77 ± 0.36	1.25 ± 0.12
F6	621.40 ± 44.09	22.23 ± 0.46	21.64 ± 0.45	1.39 ± 0.17
F7	572.06 ± 62.22	21.57 ± 0.39	21.76 ± 0.15	1.48 ± 0.16
F8	582.40 ± 16.20	21.98 ± 0.13	21.64 ± 0.44	1.35 ± 0.20
F9	564.80 ± 44.47	21.82 ± 0.57	21.80 ± 0.29	1.26 ± 0.10
F10	582.26 ± 25.21	22.40 ± 0.13	22.75 ± 0.52	1.52 ± 0.18
F11	607.93 ± 25.62	22.41 ± 0.49	21.98 ± 0.58	1.53 ± 0.12
F12	597.06 ± 68.90	22.39 ± 0.58	22.27 ± 0.18	1.49 ± 0.05
F13	520.50 ± 25.48	21.64 ± 0.28	22.07 ± 0.78	1.41 ± 0.22

2.2.3. Dimensional evaluation

Three samples were selected randomly from each 3D-printed printlet, and their length, width, and thickness were measured using a digital calliper (Fisher Scientific, UK).

2.2.4. Differential scanning calorimetry and thermogravimetric analysis

Differential scanning calorimetry (DSC) and thermogravimetric analysis (TGA) were carried out for the characterisation of the thermal properties of all materials and 3D printed formulations.

DSC analysis was performed on a DSC 214 Polyma apparatus (NETZSCH, Germany). The results were evaluated with a NETZSCH Proteus® thermal analysis software ver. 8.0 (NETZSCH, Germany), determining the glass transition behaviour and the melting and recrystallization phenomena of all raw materials and 3D printed formulations. Samples were prepared in a hermetically crimped aluminium crucible (n = 3, 5–10 mg) and a heat-cool-heat cycle was applied, analysing from −70 °C or −20 °C–80 °C in a 10 °C/min for both the heating and cooling rates.

TGA studies were conducted for the evaluation of the water content of all honey varieties. Samples (n = 3, 5–10 mg) were examined in an open aluminium pan, utilizing a Q500 TGA (TA Instruments, New Castle, DE, USA), started heating from ambient conditions to 250 °C with a 10 °C/min heating rate and an adjusted nitrogen flow rate at 40 mL/min.

2.2.5. Morphological evaluation

Surface characteristics of all honey types were examined using an optical microscope (Leica Microsystems EZ4W) under three temperature-controlled conditions: ambient (20.0 °C ± 0.5 °C), refrigerated (5.0 °C ± 0.5 °C) and (C) freezer (−20.0 °C ± 0.5 °C), to evaluate morphological differences attributed to temperature-induced crystal formation.

2.2.6. Attenuated total reflection fourier-transform infrared (ATR-FTIR) spectroscopy

ATR-FTIR spectroscopy was carried out using a Nicolet IS50 FT-IR instrument (Thermo Scientific, UK), to obtain spectra of VH, LH, JH, organic cacao, and all cacao-based printlets. The spectra were collected over the wavenumber range of 400–4000 cm^{-1} with a resolution of 4 cm^{-1}, and each sample was subjected to 32 scans.

2.2.7. Mechanical analysis

The mechanical properties of cacao-based printlets were measured at room temperature using a texture analyser (Mecmesin, MultiTest 2.5-dv, West Sussex, UK). Each cacao printlet (20 mm × 20 mm × 1 mm) was placed between 2 aluminium round-shaped platforms. Compression mode was used to analyse the samples at a compression distance of 10 mm, with a test speed of 5.0 mm/min. The measurements were conducted in triplicate and compression force was calculated.

2.2.8. Rheological studies

Rheological properties were measured using a Haake Mars rheometer (Thermo Scientific, U.K.) with a cylinder plate (P35/Ti). Measurements were initially carried out on the cacao, each variety of honey, and the cacao-based printlets. Following the printing of the printlets, measurements were taken by subjecting the 3D-printed sample to a melting process at a temperature of 32.5 °C. The gap between the plate and the stationary flatbed was set at 0.1 mm for all rheological experiments. Controlled shear rate tests were performed in the range of 0.01 s^{-1} to 700 s^{-1}. All measurements were conducted at 32.5 °C, and temperature was regulated using a circulating bath. Each experiment was performed in triplicates.

2.2.9. Disintegration testing

A disintegration test device was employed to determine the disintegration time of 3D-printed dosage forms. Three samples of each formulation were randomly selected and placed in the baskets of the disintegration test device. The baskets were immersed in 800 mL of Sodium dodecyl sulfate (SDS) buffer solution at 37 ± 2 °C and agitated in a vertical direction at a speed of 29–32 rpm.

2.2.10. Antibacterial assessment of Greek honey variants

A Clinical & Laboratory Standards Institute (CLSI) broth microdilution assay was performed to determine the MIC against *E. coli (*ATCC 25922*)* and *S. aureus* (ATCC 29213) within the range of 1–512 μl/mL via twofold serial dilutions of each honey, using sterile round bottom 96-well plates. Stock solutions of each honey were prepared aseptically in MHB. An inoculum of 1×10^6 colony forming units (CFU)/mL was prepared via a 1:100 dilution from a stock of 1×10^8 CFU/mL in MHB and 100 μl of this was added to 100 μl of each honey sample, resulting in a final concentration of 5×10^5 CFU/mL bacteria per well. A positive growth control of bacteria in MHB was prepared alongside a negative growth control of solely MHB. Plates were left for 18 h under 37 °C orbital incubation at 100 rpm. MIC was determined as the lowest concentration displaying no visual turbidity within the wells.

Determination of the MBC was performed by plating 20 μl of any wells identified as displaying no visual turbidity onto Mueller Hinton (MH) agar and spread evenly across the agar surface. Plates were statically incubated for 24 h at 37 °C to allow for bacterial growth. Plates were assessed and the MBC was determined as the lowest concentration of honey to display a 99.9 % or 3-log bacterial reduction. Experiments were performed using a 5-parallel dilution series on three independent occasions.

2.2.11. Statistical analysis

Where appropriate, data is presented as a mean ± standard deviation (SD). Statistical analysis was performed using a one-way analysis of variance (ANOVA) with Tukey's honestly significant difference (HSD) post-hoc test for the mechanical analysis results. Results were considered statistically significant were $p < 0.05$.

3. Results and discussion

3.1. Dimensional evaluation

The results provide various insights into the physical characteristics of the 3D-printed cacao-based printlets across different formulations (Table 2). Variations were observed in the weight and dimensions (length, width, and thickness) of the printlets between the formulations, indicating potential influences of the ingredients and their concentrations. Specifically, the weight of the printlets varied significantly according to the honey content. For example, formulation F13 (90% cacao, 10% JH) had a weight of 520.50 ± 25.48 mg, whereas formulation F6 (95% cacao, 5% LH) weighed 621.40 ± 44.09 mg. The weight and size of the printlets varied according to the honey content, indicating that the concentration of honey affected the printlets' physical characteristics. One potential reason for this observation is the intrinsic density and moisture content of the different types of honey used. Although honey is denser than cacao (El Sohaimy et al., 2015), the weight of the printlets may vary depending on additional factors such as material viscosity, extrusion consistency, and moisture evaporation during the printing process. Furthermore, printlets with VitD3 in addition to cacao and honey showed minor differences in weight and size from those without VitD3, highlighting the potential influence of additional ingredients. Despite these variations, consistency within each formulation group was maintained, indicating a degree of uniformity in the manufacturing process.

3.2. Thermal analysis

Thermal analysis has been conducted for all raw materials and cacao-based printlets to determine their miscibility and glass-forming attributes. These are critical for optimising the formulation process and printability studies and ensuring proper sample storage conditions.

Honey, as a supersaturated colloidal dispersion of sugars, exhibits thermally derived multi-diverse physical properties (Dettori et al., 2018). In this study, DSC analysis showed similar T_g of VH (−33.5 ± 0.7 °C), LH (−34.9 ± 1.3 °C) and JH (−34.1 ± 0.2 °C), confirming their liquid-like nature under ambient conditions (Chen et al., 2023). At freezer conditions (−20.0 ± 0.5 °C) the different honey varieties existed as semi-solid colloidal systems, prone to forming crystalline structures. Recrystallization phenomena were observed within the refrigerator temperature range (0–10 °C), due to their high sugar content (Fig. 2B). It is evident that at lower temperatures, the solubility of honey sugars is decreased, reducing the mobility of sugar molecules, and allowing carbohydrate chains to align and feasibly form crystal structures. This crystallization process is initiated by the presence of "nuclei", facilitating further crystal formation. Additionally, lower temperatures decreased water activity, which reduced the sugars' ability to remain dissolved, leading to crystallization. Contrarily, higher temperatures increased the kinetic energy of water molecules and reduced the likelihood of ice crystal formation. TGA results indicated notable stability of all honey varieties up to 38 °C ($T_{printing}$). The analysis revealed a low water content for all varieties (VH: 2.1 ± 0.1 °C, LH: 2.4 ± 0.8 °C, JH: 2.2 ± 0.2 °C) and a similar two-step degradation process ($T_{deg} \approx$ 120 °C) (Table S2), attributed to their common plant species origins (Dimitriu et al., 2022) (Fig. 2A).

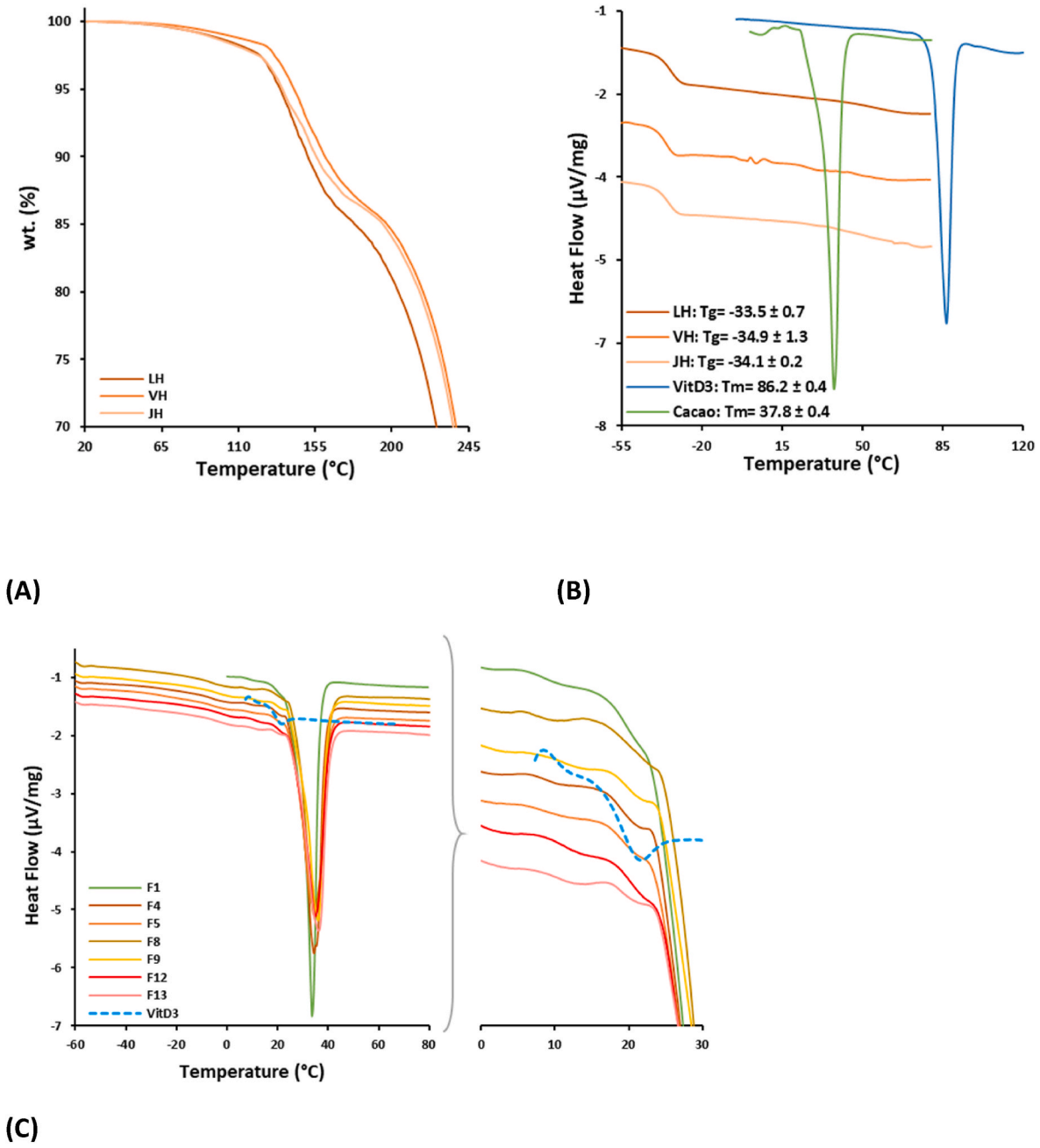

Fig. 2. Thermograms depicting the (A) degradation behaviour of all honey varieties, (B) glass transition temperature of all raw materials and (C) melting behaviour of all VitD3 loaded 3D printed formulations, superimposed to highlight their different T_g. F1 is the control (cacao) without honey and vitD3.

Moreover, VitD3 (T_m = 86.2 ± 0.4 °C) proved to amorphise after undergoing a heat-cool-heat cycle (T_g = 19.9 ± 0.1 °C), demonstrating its capability to form glass structures (Jelić et al., 2024). Therefore, VitD3 was incorporated into melted cacao (T ~ 80 °C) and gently mixed for 5 min to ensure its complete dissolution in the melted mixture and its subsequent amorphization. Thermal analysis confirmed the presence of the amorphous state of VitD3 in all cacao/honey formulations (F4: 8.6 ± 0.1 °C, F5: 7.5 ± 0.8 °C, F8: 8.7 ± 1.4 °C, F9: 10.5 ± 0.2 °C, F12: 11.0 ± 0.2 °C, F13: 8.7 ± 0.9 °C), which is slightly lower comparably to the raw VitD3 probably due to the presence of both cacao and honey in the formulation, proving its efficient miscibility within the composite inks (Gupta et al., 2018) (Fig. 2C).

The determination of T_g was crucial not only for optimising the formulation and printing process, but also for ensuring appropriate sample storage conditions. Optical microscopy observations indicated that LH maintained a consistent viscous liquid state, while lower temperatures impacted the crystal formation in both VH and JH (Fig. 3). Moreover, the onset melting point and the different glass transition (Tg) values observed in the cacao-based printed formulations demonstrate their thermal behaviour and stability under various conditions. DSC studies, which prove the presence of Tg (VitD3) into the printlets (see Table S1) necessitated storage at refrigerator temperatures (0–5 °C), to maintain the stability of the printed forms. Overall, honey and VitD3 were efficiently dissolved into the cacao matrices, and cacao was noted as an efficient nutrient carrier, exhibiting reproducible thermal behaviour after being printed, stored under refrigeration and subsequently re-exposed to ambient temperature (Calva-Estrada et al., 2020).

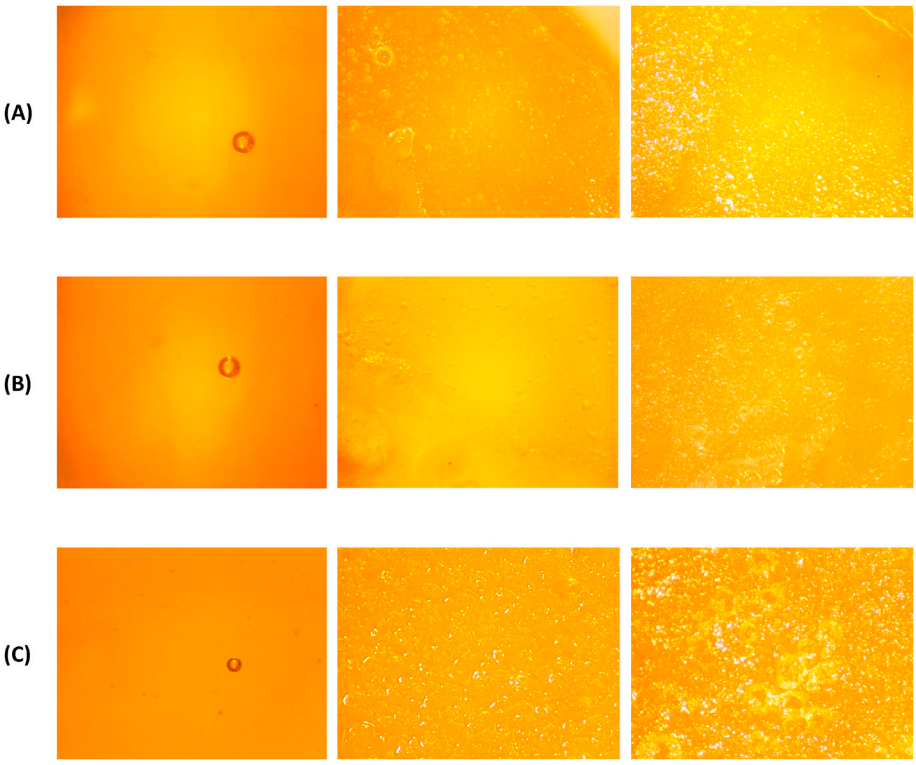

Fig. 3. Optical microscopy images depicting the physical characteristics – surface morphology and colour–, of the different honey varieties (LH, VH, and JH) under three storage conditions: (A) ambient (20.0 °C ± 0.5 °C), (B) refrigerated (5.0 °C ± 0.5 °C) and (C) freezer temperature (−20.0 °C ± 0.5 °C).

3.3. ATR-FTIR spectroscopy

The ATR-FTIR spectroscopic analysis of the raw materials and cacao printlets reveals unique characteristic bonding patterns (Fig. 4). A band at around 3500 cm^{-1} may be seen in the organic cacao and cacao-based printlets, which is suggestive of O-H stretching. The presence of this O-H stretching band in both organic cacao and cacao-based printlets is indicative of hydroxyl groups. These hydroxyl groups are commonly associated with compounds such as phenols, alcohols, or water molecules. This band may result from the inherent moisture content of organic cacao as well as the presence of polyphenolic chemicals in cacao-based inks (Deus et al., 2021). Interestingly, upon the inclusion of LH, VH or JH honey varieties, minimal changes were observed in the absorption bands. Although slight changes in the molecular environment were observed, these may indicate hydrogen bonding interactions between flavonoids and other substances present in the cacao and honey matrix (Zheng et al., 2016), these changes were not pronounced enough to induce substantial chemical alterations in the cacao-based printlet structure.

The bands at approximately 2915 cm^{-1} and 2849 cm^{-1} are attributable to C-H stretching within the aromatic ring. These bands suggest the prevalence of aromatic compounds, possibly derived from the cacao solids present in chocolate. The aromatic ring stretching vibrations are integral components of compounds like polyphenols and flavonoids, contributing to the characteristic flavour and aroma of cacao (Shen et al., 2022). The consistency of these bands across all cacao-based samples suggests a uniformity in the cacao matrix. Notably, all cacao samples exhibit the methylene group band at 1471 cm^{-1} and the C=O stretching mode at 1730 cm^{-1} (Grillo et al., 2019), which together offer important insights into the general characterisation of cacao-based ink. The C=O stretching mode is typically associated with carbonyl groups, indicating the presence of lipids or fats in cacao. This result aligns with the expected composition of cacao, which includes triglyceride-containing cacao butter. The methylene group band, located at 1471 cm^{-1}, supports the evidence for the presence of lipids, particularly the -CH_2 groups found in cacao butter (Ghazani and Marangoni, 2021).

The ATR FTIR analysis of the three honey types, LH, VH, and JH, shows distinct vibrational patterns. In the LH spectrum, vibrational modes include the C-H bond stretching at 2931 cm^{-1} and the O-H bending mode associated with water at 1640 cm^{-1} (Anjos et al., 2021). Honey presence is marked by absorption bands between 1421 and 1151 cm^{-1}, revealing bending modes of C-C-H, C-O-H, and O-C-H groups, these could indicate the presence of sugars or carbohydrates in the honey (Nguyen et al., 2018). Similarly, VH and JH spectra display the C-H bond at 2930 cm^{-1} and 2931 cm^{-1}, respectively, and the O-H bending mode at 1644 cm^{-1} and 1647 cm^{-1}. Distinct honey absorption bands appear between 1345 and 1023 cm^{-1} in both spectra, with a significant absorbance band within the 1147-918 cm^{-1} range attributed to deformations of O–H, C–O, C–H, and C=C bonds, which are characteristic of phenolic compounds and carbohydrates in honey (Ganaie et al., 2021).

The VitD3 spectrum shows several distinct bands. The presence of an O–H bond is demonstrated by the signal at 3291 cm^{-1}. The C–H vibrations correspond to the band at 2933 cm^{-1}. The presence of a C=C bond is confirmed by the band at 1634 cm^{-1}. Additionally, the signals observed at approximately 1457 cm^{-1} are associated with deformation vibrations of -CH2, while those at 1376 cm^{-1} indicate deformation vibrations of the -CH3 chemical moiety (Jannasari et al., 2019). The band observed at 1053 cm^{-1} corresponds to the C-O groups present in the sample, and the region between 834 and 967 cm^{-1} can be attributed to C-H vibrations. Furthermore, a weak peak at 717 cm^{-1} is also observed, corresponding to the weak tensile vibration of the -CH2 group.

3.4. Mechanical analysis

The texture analysis results for the various formulations, each containing different percentages of each of the honey varieties, cacao, and

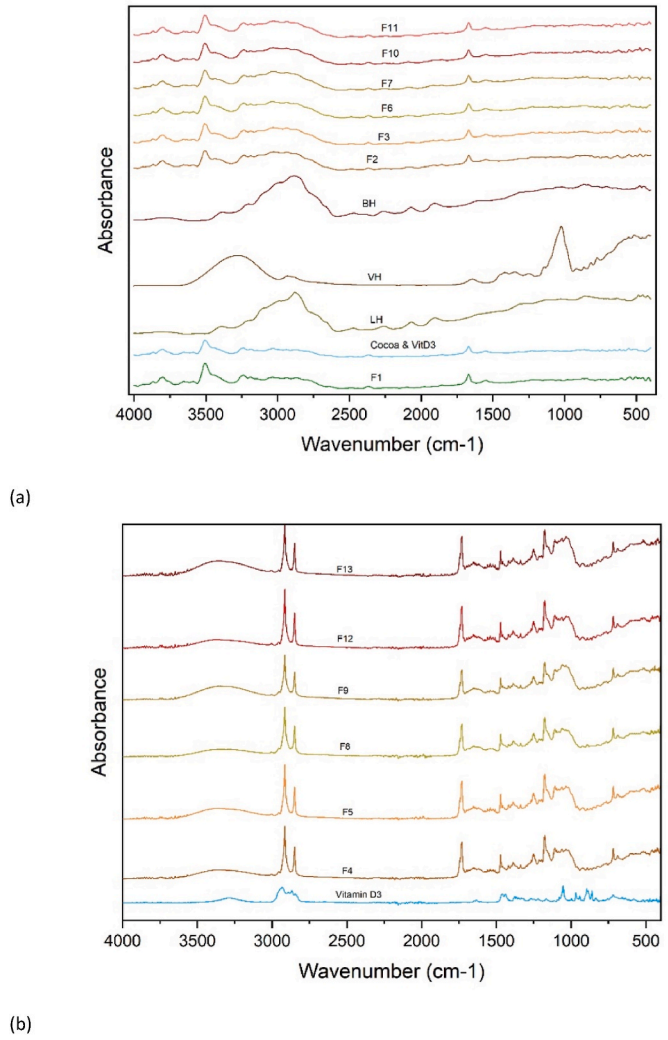

Fig. 4. FTIR spectra of (A) raw materials and cacao-based printlets and (B) VitD3 and VitD3-loaded cacao-based formulations.

VitD3, are summarized in Table 3. Each formulation's deformation was measured in terms of force (N) and distance (mm). The analysis shows that the type and concentration of honey influence the textural properties of the printlets. JH generally increased firmness, as evidenced by the higher forces required for formulations containing JH. For example, formulation F10 required a force of 6.23 ± 3.24 N for compression, significantly higher compared to formulations like F2, which required 3.40 ± 0.92 N, and F8, which required 3.97 ± 0.29 N. LH-based printlets, especially at 5% w/w, showed significant increases in firmness,

Table 3
Mechanical properties breaking force of the 3D printed Cacao printlets.

Formulations	Force (N)	Distance (MM)
F2	3.40 ± 0.92	0.91 ± 0.59
F3	5.43 ± 2.50	0.90 ± 0.49
F4	3.33 ± 3.21	0.68 ± 0.75
F5	4.27 ± 0.73	0.44 ± 0.19
F6	11.86 ± 0.74	1.33 ± 0.05
F7	0.13 ± 0.05	0.22 ± 0.17
F8	3.97 ± 0.29	0.46 ± 0.25
F9	6.07 ± 5.86	0.76 ± 0.79
F10	6.23 ± 3.24	1.18 ± 0.86
F11	3.76 ± 3.11	0.27 ± 0.05
F12	3.97 ± 1.08	1.02 ± 0.93
F13	1.10 ± 0.83	2.31 ± 2.46

with F6 being the firmest formulation tested, requiring a force of 11.86 ± 0.74 N for compression. However, the addition of VitD3 to JH formulations introduced variability, reducing firmness and increasing distance in F13 compared to F12. This variation raises the possibility of problems with material distribution or mixing techniques impacting texture consistency. Furthermore, the addition of VitD3 tended to increase variability in both force and distance measurements, indicating potential interactions with other formulation components that compromise structural integrity. In the context of nutraceuticals firmness is a critical parameter as it affects both the mechanical stability and the release profile of the active ingredients (Adeleye, 2019). Printlets must be firm enough to hold their shape during handling and storage, but too much hardness can prevent the product from releasing and disintegrating, which could reduce its effectiveness or even unpalatable (Faccinetto-Beltrán et al., 2021).

Statistical analysis revealed that there is no significant difference in both force and distance among the various formulations tested ($p > 0.05$ for all comparisons) (Tables 3a, 3b, 3c and 3d-supplementary material). This indicates that neither force nor distance is significantly influenced by the choice of formulation in our study. It has been previously reported that mechanical properties such as hardness, strength, flexibility, and texture can be influenced by factors such as filling percentage, filling pattern, sample shape, and even the measurement direction, in addition to formulation composition (Tejada-Ortigoza and Cuan-Urquizo, 2022). Therefore, the mechanical properties obtained will depend on the specific selection of measurement parameters. Further optimization is required to ensure that the incorporation of VitD3 does not cause any detrimental effects on the integrity of the cacao-based printlets. Overall, the texture analysis in this study shows how important honey type, concentration, and VitD3 addition are to the formulations' firmness and elasticity.

3.5. Rheological analysis

Fig. 5 (a, b, and c) presents the rheological results for the raw honey, cacao and 3D cacao-based printlets loaded and unloaded with VitD3. The flow behaviour of the blank and the VitD3-loaded cacao-based printlets was evaluated to determine the extrusion temperature during the 3D Printing process. Each of the raw honey samples showed Newtonian fluid behaviour (Faustino and Pinheiro, 2021) this was characterized by constant viscosity at the fixed temperature of 32.5 °C. Most of the cacao-based printlets displayed consistent rheological behaviour, characterized by a decrease in viscosity as the shear rate increased from 0.01 s^{-1} to 100 s^{-1} at 32.5 °C, indicative of pseudoplastic flow behaviour. This behaviour is desirable for the extrusion of cacao-based inks from the printer nozzle. These findings align with previous studies, which have also reported similar rheological behaviour in cacao-based materials used for 3DP applications (Karyappa and Hashimoto, 2019). The observed variations in rheological behaviour upon the addition of LH honey at different concentrations, both with and without VitD3, can be influenced by several factors. Firstly, changes in honey concentration affect the rheological properties by altering the material composition, which influences interactions and structural arrangements. For example, the viscosity of VitD3-loaded chocolate ink with 10% LH is 0.06676 Pas at a high shear rate of 699.95 s^{-1}. A lower shear rate of 0.00864 s^{-1} increases significantly to 46.47 Pas. Similarly, for the VitD3-loaded chocolate ink with 5% LH, the viscosity increases from 0.140387 Pas at 699.95 s^{-1}–46.47 Pas at 0.00864 s^{-1}, and for raw LH, it increases from 3.343 Pas to 5.829333 Pas over the same range. These changes highlight the non-Newtonian, shear-thinning behaviour of LH, where the viscosity decreases with increasing shear rate. Secondly, the introduction of VitD3 may interact synergistically with honey and chocolate, further modifying the mixture's microstructure and flow properties (Oroian et al., 2016). Secondly, the particle size distribution should be considered, as it impacts the rheological behaviour of the mixture (Feichtinger et al., 2020). Overall, the concentration of honey, the presence of VitD3, and

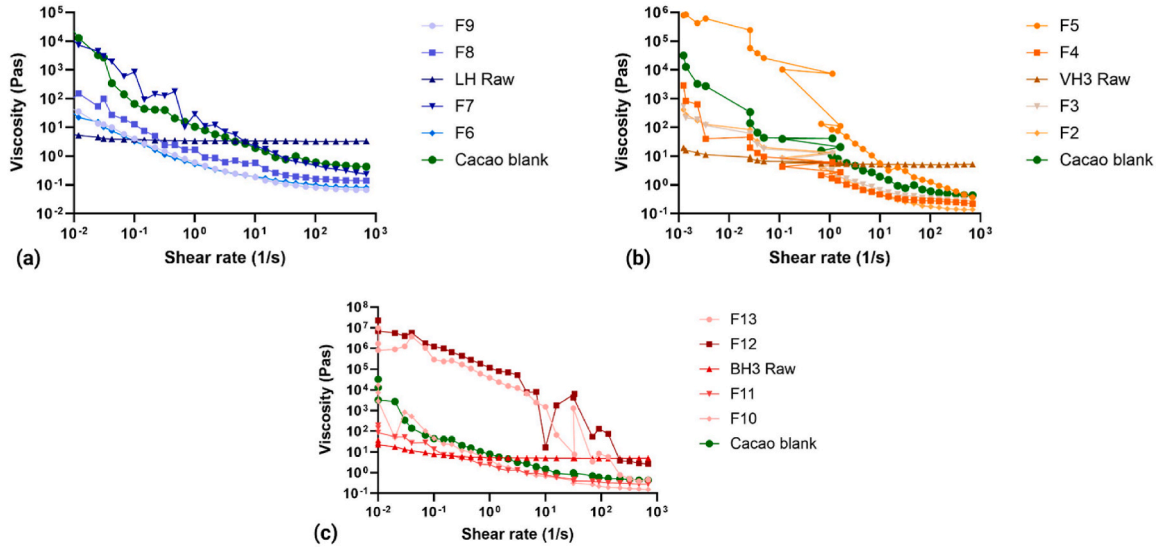

Fig. 5. Rheological analysis results of (a) LH, cacao blank, VitD3 loaded chocolate printlets; (b) VH, cacao blank, VitD3 loaded cacao-based printlets; (c) JH, cacao blank and VitD3 loaded cacao-based printlets. The results represent the mean values of measurements run in triplicate. Error bars have been removed for clarity.

particle size distribution are key factors influencing the rheological properties of the mixture.

The rheological analysis of the cacao blends with varying concentrations of VH and JH presented intriguing findings. At a 5% concentration of VH and JH, the cacao blend exhibited the lowest viscosity; however, the rheological profile presented fluctuations, characterized by non-linear variations in viscosity across shear rates. This behaviour suggests a lack of consistency in the fluid's response to shear, furthermore, the addition of VitD3 to the 5% honey concentrations led to a slight increase in viscosity, indicating a potential interaction effect between both honey and VitD3 components. Interestingly, at a 10% concentration of both types of honey, similar rheological trends were observed compared to the 5%. Overall, the results from the JH parallel those from the VH blends, suggesting common underlying mechanisms governing rheological behaviour in honey-infused cacao blends. Further investigations into these mechanisms are warranted to elucidate the intricate molecular interactions influencing the observed rheological responses.

3.6. Disintegration testing

Based on the results of the disintegration experiment, all printlets successfully disintegrated within 30 min. Notably, formulations with a higher percentage of honey took slightly longer to disintegrate compared to those with a lower honey content. For instance, printlets containing 10% honey disintegrated in an average of 15 min, while those with 5% honey disintegrated in approximately 13 min. This indicates that higher honey content slightly slows down the disintegration process, likely due to the increased viscosity and cohesive properties imparted by the honey (Tappi et al., 2021). Furthermore, printlets containing VitD3 required more time to disintegrate than those without VitD3. Specifically, printlets with VitD3 and 10% honey disintegrated in about 30 min, compared to 15 min for those with 10% honey but without VitD3. These observations suggest that both the concentration of honey and the inclusion of VitD3 influence the disintegration time of the printlets. The lipid-soluble nature of VitD3 may enhance the hydrophobic characteristics of the printlets, increasing their resistance to water absorption and delaying the disintegration process. The slightly longer disintegration times for formulations with higher honey content and VitD3 provide additional advantages. The extended disintegration times can contribute to a more controlled release of VitD3. Additionally, the inclusion of honey enhances taste and delays disintegration, making the printlets more palatable and acceptable, especially for children and those with taste sensitivities (Palma-Morales et al., 2023). Honey's higher viscosity and binding qualities (Aga et al., 2023), combined with VitD3's hydrophobic qualities (Żurek et al., 2023), may enhance the printlets' structural stability, beneficial during handling, packaging, and transportation, reducing the risk of breakage. Overall, the disintegration times observed in this study indicate that the 3D-printed chocolate-based printlets are suitable for delivering VitD3, offering potential benefits in controlled release, palatability, stability, and patient adherence.

3.7. Bacterial studies

The determined MIC and MBC values (Table 4 and Table S5 supplementary material) effectively inhibited the growth of Gram-positive bacteria, *Staphylococcus aureus (S. aureus)* and Gram-negative bacteria *Escherichia coli. (E. coli*). For *S. aureus*, the MIC values were 4 μL/mL under LH, 8 μL/mL under VH, and 8 μL/mL under JH For *E. coli*, the corresponding MIC values were 16 μL/mL across LH, VH, and JH conditions. The MBC values were calculated across a range of honey concentrations, and each concentration demonstrated a reduction in bacterial load of ≥99.9% from the initial 5×10^5 CFU/mL stock solution. The MBC results are summarized in Table S5, which shows strong bactericidal activity against *S. aureus* and *E. coli* at all tested concentrations. Among them, LH indicated a greater potency in antibacterial activity, achieving MIC values of 4 μL/mL for *S. aureus* and 16 μL/mL for E. *coli*, respectively, indicating a significant inhibitory effect at a low concentration (10% w/v). These values fall short of those observed in the literature, where MIC values for lavender honey have been reported as 12.5–25% (Sakač et al., 2022) and 10–25% (Osés et al., 2024). This disparity could be caused by several things, including changes in the

Table 4
MIC limits were determined for each of the raw honey via visual inspection of wells after 24 h of incubation.

	S. aureus	E– coli
LH	4 μL/mL	16 μL/mL
VH	8 μL/mL	16 μL/mL
BH	8 μL/mL	16 μL/mL

honey's processing, storage, and botanical origin, as well as methodological variances in the MIC determination. Furthermore, our study's strains of *S. aureus* and *E. coli* might not be the same as those utilised in earlier studies, which could affect the MIC values that were found. Despite these differences, our results show high activity at comparatively low doses, which is consistent with the overall antibacterial efficacy of lavender honey documented in the literature.

This finding aligns with current literature, underscoring the effectiveness of LH in combating bacterial growth. In addition to determining MIC and MBC values, the disk diffusion method (Figs. S2 and S3-supplementary material) was used to further evaluate the antibacterial efficacy of the chocolate honey printlets. However, no zones of inhibition were observed after 24 h and 48 h of incubation. Several factors could have contributed to this outcome. It is possible that the concentration of active antibacterial compounds in the chocolate honey printlets was insufficient, hindering their ability to produce a measurable zone of inhibition, previous reports have suggested many honey variants require concentrations of 15–80 % w/v are necessary to observe visible inhibitory zones against pathogenic bacteria (Albaridi, 2019; Obey et al., 2022). Alternatively, the diffusion properties of the active compounds might have been compromised, potentially due to the viscosity of the printlet or the presence of interfering substances. Additionally, it's possible that some elements of the chocolate honey printlets had an interaction with the bacterial cells or agar medium, which changed the outcome. It should be noted however that bacterial growth was not observed where the sample had been in contact with the agar after it was removed. Contact kill is a phenomenon that indicates that an antimicrobial agent can still have an antibacterial effect when it comes into direct touch with bacteria, even if it does not disperse into the agar to form a visible zone (Balouiri et al., 2016). Future studies could explore modifying ink formulations, testing a broader range of bacterial strains, and assessing the stability of the ink under different storage conditions to better understand and optimize their antibacterial properties.

4. Conclusion

In this current study, the feasibility of utilizing cacao-based formulations infused with honey for 3D printing applications was effectively demonstrated, with a specific focus on incorporating bioactive compounds such as VitD3. The physicochemical and thermal analyses confirmed that the addition of the three different honey varieties preserved the molecular integrity and desired properties of the cacao printlets. Thermal analysis demonstrated that all honey types maintain a liquid-like nature under ambient conditions and their stability was maintained up to the printing temperature of 38 °C. Furthermore, the amorphous integration of VitD3 within the chocolate matrix ensured uniform distribution and enhanced stability. Rheological evaluations revealed that the raw honey samples exhibited Newtonian fluid behaviour, whereas the chocolate inks displayed pseudoplastic flow behaviour, which is advantageous for the extrusion process in 3D printing. The observed increase in viscosity with higher honey concentrations and the presence of VitD3 suggest that the rheological properties of the formulations can be tailored to enhance printability and structural integrity.

Among the honey varieties tested, LH at a 10% w/w concentration emerged as the optimal formulation. Beyond enhancing structural integrity and thermal stability, LH is hypothesized to improve palatability due to honey's natural sweetness and flavour-enhancing properties, which are pivotal for enhancing patient adherence and product acceptability in therapeutic applications. However, this remains speculative in the absence of sensory analysis, which should be addressed in future studies. Moreover, honey's documented effects on nutrient release, as evidenced by disintegration and dissolution tests, underscore its multifaceted role beyond its inherent sweetness. The findings of this study highlight the potential of 3DP Cacao-based printlets as innovative delivery systems for bioactive compounds. The use of honey not only enhances the structural and thermal properties but also its palatability and potential nutrient release modulation. These formulations harness the immune-boosting properties of VitD3 and honey, demonstrating how 3DP technology can innovate personalized health solutions. This approach not only enhances patient adherence and palatability but also underscores the versatility of 3DP in developing customized health supplements and nutraceuticals.

CRediT authorship contribution statement

Rachel L. Milliken: Conceptualization, Data curation, Formal analysis, Methodology, Investigation, Writing – original draft, Writing – review & editing. **Aikaterini Dedeloudi:** Data curation, Methodology, Investigation, Writing – review & editing. **Emily Vong:** Conceptualization, Data curation, Formal analysis, Methodology, Investigation, Writing – original draft, Writing – review & editing. **Robyn Irwin:** Conceptualization, Data curation, Formal analysis, Methodology, Investigation, Writing – original draft, Writing – review & editing. **Sune K. Andersen:** Supervision, Writing – review & editing. **Matthew P. Wylie:** Conceptualization, Methodology, Funding acquisition, Supervision, Writing – review & editing. **Dimitrios A. Lamprou:** Conceptualization, Methodology, Funding acquisition, Supervision, Writing – review & editing.

Data statement

Upon request to the authors, all data for this project can be made freely available.

Sources of funding

E.V. summer project sponsored by the School of Pharmacy at Queen's University Belfast.

Declaration of competing interest

The authors declare that they have no known competing financial interests or personal relationships that could have appeared to influence the work reported in this paper.

Appendix A. Supplementary data

Supplementary data to this article can be found online at https://doi.org/10.1016/j.crfs.2024.100949.

Data availability

Data will be made available on request.

References

Adeleye, O.A., 2019. Relationship between compression pressure, mechanical strength and release properties of tablets. Polim. Med. 49, 27–33. https://doi.org/10.17219/pim/111888.

Aga, M.B., Sharma, V., Dar, A.H., Dash, K.K., Singh, A., Shams, R., Khan, S.A., 2023. Comprehensive review on functional and nutraceutical properties of honey. eFood 4, e71. https://doi.org/10.1002/efd2.71.

Albaridi, N.A., 2019. Antibacterial potency of honey. Internet J. Microbiol. 2019, 2464507. https://doi.org/10.1155/2019/2464507.

Anjos, O., Guiné, R.P.F., Santos, A.J.A., Paula, V.B., Pereira, H., Estevinho, L.M., 2021. Evaluation of FT-Raman and FTIR-ATR spectroscopy for the quality evaluation of Lavandula spp. Honey. Open Agric 6, 47–56. https://doi.org/10.1515/opag-2020-0210.

Balouiri, M., Sadiki, M., Ibnsouda, S.K., 2016. Methods for *in vitro* evaluating antimicrobial activity: a review. J. Pharm. Anal. 6, 71–79. https://doi.org/10.1016/j.jpha.2015.11.005.

Benelam, B., Wiseman, M., 2019. Size matters: developing portion size guidance for consumers. Nutr. Bull. 44, 4–6. https://doi.org/10.1111/nbu.12360.

Bizerra, F.C., Da Silva Junior, P.I., Hayashi, M.A., 2012. Exploring the antibacterial properties of honey and its potential. Front. Microbiol. 3. https://doi.org/10.3389/fmicb.2012.00398.

Brudzynski, K., 2020. A current perspective on hydrogen peroxide production in honey. A review. Food Chem. 332, 127229. https://doi.org/10.1016/j.foodchem.2020.127229.

Brudzynski, K., Abubaker, K., Castle, A., 2011. Re-examining the role of hydrogen peroxide in bacteriostatic and bactericidal activities of honey. Front. Microbiol. 2. https://doi.org/10.3389/fmicb.2011.00213.

Calva-Estrada, S.J., Utrilla-Vázquez, M., Vallejo-Cardona, A., Roblero-Pérez, D.B., Lugo-Cervantes, E., 2020. Thermal properties and volatile compounds profile of commercial dark-chocolates from different genotypes of cocoa beans (*Theobroma cacao* L.) from Latin America. Food Res. Int. 136, 109594. https://doi.org/10.1016/j.foodres.2020.109594.

Chachlioutaki, K., Karavasili, C., Mavrokefalou, E.-E., Gioumouxouzis, C.I., Ritzoulis, C., Fatouros, D.G., 2022. Quality control evaluation of paediatric chocolate-based dosage forms: 3D printing vs mold-casting method. Int. J. Pharm. 624, 121991. https://doi.org/10.1016/j.ijpharm.2022.121991.

Chen, L., Huang, S., Ras, R.H.A., Tian, X., 2023. Omniphobic liquid-like surfaces. Nat. Rev. Chem 7, 123–137. https://doi.org/10.1038/s41570-022-00455-w.

Dettori, A., Tappi, S., Piana, L., Dalla Rosa, M., Rocculi, P., 2018. Kinetic of induced honey crystallization and related evolution of structural and physical properties. Lebensm. Wiss. Technol. 95, 333–338. https://doi.org/10.1016/j.lwt.2018.04.092.

Deus, V.L., Resende, L.M., Bispo, E.S., Franca, A.S., Gloria, M.B.A., 2021. FTIR and PLS-regression in the evaluation of bioactive amines, total phenolic compounds and antioxidant potential of dark chocolates. Food Chem. 357, 129754. https://doi.org/10.1016/j.foodchem.2021.129754.

El Sohaimy, S.A., Masry, S.H.D., Shehata, M.G., 2015. Physicochemical characteristics of honey from different origins. Ann. Agric. Sci. 60, 279–287. https://doi.org/10.1016/j.aoas.2015.10.015.

Eswaran, H., Ponnuswamy, R.D., Kannapan, R.P., 2023. Perspective approaches of 3D printed stuffs for personalized nutrition: a comprehensive review. Ann. 3D Print. Med 12, 100125. https://doi.org/10.1016/j.stlm.2023.100125.

Faccinetto-Beltrán, P., Gómez-Fernández, A.R., Santacruz, A., Jacobo-Velázquez, D.A., 2021. Chocolate as carrier to deliver bioactive ingredients: current advances and future perspectives. Foods 10, 2065. https://doi.org/10.3390/foods10092065.

Faustino, C., Pinheiro, L., 2021. Analytical rheology of honey: a state-of-the-art review. Foods 10, 1709. https://doi.org/10.3390/foods10081709.

Feichtinger, A., Scholten, E., Sala, G., 2020. Effect of particle size distribution on rheological properties of chocolate. Food Funct. 11, 9547–9559. https://doi.org/10.1039/D0FO01655A.

Ganaie, T.A., Masoodi, F.A., Rather, S.A., Wani, S.M., 2021. Physicochemical, antioxidant and FTIR-ATR spectroscopy evaluation of Kashmiri honeys as food quality traceability and Himalayan brand. J. Food Sci. Technol. 58, 4139–4148. https://doi.org/10.1007/s13197-020-04878-5.

Grillo, G., Boffa, L., Binello, A., Mantegna, S., Cravotto, G., Chemat, F., Dizhbite, T., Lauberte, L., Telysheva, G., 2019. Analytical dataset of Ecuadorian cocoa shells and beans. Data Brief 22, 56–64. https://doi.org/10.1016/j.dib.2018.11.129.

Gupta, R., Behera, C., Paudwal, G., Rawat, N., Baldi, A., Gupta, P.N., 2018. Recent advances in formulation strategies for efficient delivery of vitamin D. AAPS PharmSciTech 20, 11. https://doi.org/10.1208/s12249-018-1231-9.

Halib, H., Ismail, A., Yusof, B.-N.M., Osakabe, N., Daud, Z.A.M., 2020. Effects of cocoa polyphenols and dark chocolate on obese adults: a scoping review. Nutrients 12, 3695. https://doi.org/10.3390/nu12123695.

Jannasari, N., Fathi, M., Moshtaghian, S.J., Abbaspourrad, A., 2019. Microencapsulation of vitamin D using gelatin and cress seed mucilage: production, characterization and *in vivo* study. Int. J. Biol. Macromol. 129, 972–979. https://doi.org/10.1016/j.ijbiomac.2019.02.096.

Jerusalem Sage [WWW Document], n.d. URL https://specialtyproduce.com/produce/Jerusalem_Sage_10537.php (accessed 6.26.24).

Kamal, N., Mio Asni, N.S., Rozlan, I.N.A., Mohd Azmi, M.A.H., Mazlan, N.W., Mediani, A., Baharum, S.N., Latip, J., Assaw, S., Edrada-Ebel, R.A., 2022. Traditional medicinal uses, phytochemistry, biological properties, and health applications of Vitex sp. Plants 11, 1944. https://doi.org/10.3390/plants11151944.

Karavasili, C., Gkaragkounis, A., Moschakis, T., Ritzoulis, C., Fatouros, D.G., 2020. Pediatric-friendly chocolate-based dosage forms for the oral administration of both hydrophilic and lipophilic drugs fabricated with extrusion-based 3D printing. Eur. J. Pharmaceut. Sci. 147, 105291. https://doi.org/10.1016/j.ejps.2020.105291.

Karyappa, R., Hashimoto, M., 2019. Chocolate-based ink three-dimensional printing (Ci3DP). Sci. Rep. 9, 14178. https://doi.org/10.1038/s41598-019-50583-5.

Lester, S., Kleijn, M., Cornacchia, L., Hewson, L., Taylor, M.A., Fisk, I., 2022. Factors affecting adherence, intake, and perceived palatability of oral nutritional supplements: a literature review. J. Nutr. Health Aging 26, 663–674. https://doi.org/10.1007/s12603-022-1819-3.

Nguyen, H.T.L., Panyoyai, N., Paramita, V.D., Mantri, N., Kasapis, S., 2018. Physicochemical and viscoelastic properties of honey from medicinal plants. Food Chem. 241, 143–149. https://doi.org/10.1016/j.foodchem.2017.08.070.

Obey, J.K., Ngeiywa, M.M., Lehesvaara, M., Kauhanen, J., von Wright, A., Tikkanen-Kaukanen, C., 2022. Antimicrobial activity of commercial organic honeys against clinical isolates of human pathogenic bacteria. Org. Agric. For. 12, 267–277. https://doi.org/10.1007/s13165-022-00389-z.

Office of Dietary Supplements - Vitamin D [WWW Document], n.d. URL https://ods.od.nih.gov/factsheets/VitaminD-Consumer/(accessed 6.27.24).

Oracz, J., Żyżelewicz, D., 2020. Antioxidants in cocoa. Antioxidants 9, 1230. https://doi.org/10.3390/antiox9121230.

Oroian, M., Paduret, S., Amariei, S., Gutt, G., 2016. Chemical composition and temperature influence on honey texture properties. J. Food Sci. Technol. 53, 431–440. https://doi.org/10.1007/s13197-015-1958-1.

Osés, S.M., Rodríguez, C., Valencia, O., Fernández-Muiño, M.A., Sancho, M.T., 2024. Relationships among hydrogen peroxide concentration, catalase, glucose oxidase, and antimicrobial activities of honeys. Foods 13, 1344. https://doi.org/10.3390/foods13091344.

Palma-Morales, M., Huertas, J.R., Rodríguez-Pérez, C., 2023. A comprehensive review of the effect of honey on human health. Nutrients 15, 3056. https://doi.org/10.3390/nu15133056.

Parham, S., Kharazi, A.Z., Bakhsheshi-Rad, H.R., Nur, H., Ismail, A.F., Sharif, S., RamaKrishna, S., Berto, F., 2020. Antioxidant, antimicrobial and antiviral properties of herbal materials. Antioxidants 9, 1309. https://doi.org/10.3390/antiox9121309.

Parker, G., Parker, I., Brotchie, H., 2006. Mood state effects of chocolate. J. Affect. Disord. 92, 149–159. https://doi.org/10.1016/j.jad.2006.02.007.

Pressman, P., Clemens, R.A., Hayes, A.W., 2017. Bioavailability of micronutrients obtained from supplements and food: a survey and case study of the polyphenols. Toxicol. Res. Appl. 1, 2397847317696366. https://doi.org/10.1177/2397847317696366.

Ramesh, P., Jagadeesan, R., Sekaran, S., Dhanasekaran, A., Vimalraj, S., 2021. Flavonoids: classification, function, and molecular mechanisms involved in bone remodelling. Front. Endocrinol. 12, 779638. https://doi.org/10.3389/fendo.2021.779638.

Sakač, M., Jovanov, P., Marić, A., Četojević-Simin, D., Novaković, A., Plavšić, D., Škrobot, D., Kovač, R., 2022. Antioxidative, antibacterial and antiproliferative properties of honey types from the western balkans. Antioxidants 11, 1120. https://doi.org/10.3390/antiox11061120.

Scholey, A., Owen, L., 2013. Effects of chocolate on cognitive function and mood: a systematic review. Nutr. Rev. 71, 665–681. https://doi.org/10.1111/nure.12065.

Shen, N., Wang, T., Gan, Q., Liu, S., Wang, L., Jin, B., 2022. Plant flavonoids: classification, distribution, biosynthesis, and antioxidant activity. Food Chem. 383, 132531. https://doi.org/10.1016/j.foodchem.2022.132531.

Šimoliūnas, E., Rinkūnaitė, I., Bukelskienė, Ž., Bukelskienė, V., 2019. Bioavailability of different vitamin D oral supplements in laboratory animal model. Medicina (Mex.) 55, 265. https://doi.org/10.3390/medicina55060265.

Synaridou, M.S., Morichovitou, A.K., Markopoulou, C.K., 2020. Innovative pediatric formulations: ibuprofen in chocolate-coated honey core. J. Pharm. Innov. 15, 404–415. https://doi.org/10.1007/s12247-019-09389-1.

Tappi, S., Glicerina, V., Ragni, L., Dettori, A., Romani, S., Rocculi, P., 2021. Physical and structural properties of honey crystallized by static and dynamic processes. J. Food Eng. 292, 110316. https://doi.org/10.1016/j.jfoodeng.2020.110316.

Tejada-Ortigoza, V., Cuan-Urquizo, E., 2022. Towards the development of 3D-printed food: a rheological and mechanical approach. Foods 11, 1191. https://doi.org/10.3390/foods11091191.

Ullah, A., Munir, S., Badshah, S.L., Khan, N., Ghani, L., Poulson, B.G., Emwas, A.-H., Jaremko, M., 2020. Important flavonoids and their role as a therapeutic agent. Molecules 25, 5243. https://doi.org/10.3390/molecules25225243.

Waterhouse, A.L., Shirley, J.R., Donovan, J.L., 1996. Antioxidants in chocolate. Lancet 348 (9030), 834. https://doi.org/10.1016/S0140-6736(05)65262-2.

Weaver, E., O'Hagan, C., Lamprou, D.A., 2022. The sustainability of emerging technologies for use in pharmaceutical manufacturing. Expet Opin. Drug Deliv. 19, 861–872. https://doi.org/10.1080/17425247.2022.2093857.

Zheng, Y.-Z., Zhou, Y., Liang, Q., Chen, D.-F., Guo, R., 2016. Theoretical studies on the hydrogen-bonding interactions between luteolin and water: a DFT approach. J. Mol. Model. 22, 257. https://doi.org/10.1007/s00894-016-3128-4.

Żurek, G., Przybyło, M., Witkiewicz, W., Langner, M., 2023. Novel approach for the approximation of vitamin D3 pharmacokinetics from in vivo absorption studies. Pharmaceutics 15, 783. https://doi.org/10.3390/pharmaceutics15030783.